

THE EFFECT OF CATION SUBSTITUTIONS ON THE PHYSICAL PROPERTIES OF TRIOCTAHEDRAL MICAS

ROBERT M. HAZEN AND DAVID R. WONES,¹ *Department of Earth
and Planetary Sciences, Massachusetts Institute of Technology
Cambridge, Massachusetts 02139*

ABSTRACT

Unit cell dimensions and refractive indices have been determined for synthetic hydrous trioctahedral micas in which each of Co^{2+} , Cu^{2+} , Fe^{2+} and Ni^{2+} completely occupies the octahedral sites. Zn- and Mn-micas with excess aluminum have also been synthesized, but syntheses of pure Zn^{2+} , Mn^{2+} , Cd^{2+} , and Pb^{2+} micas were not successful. Tetrahedral substitutions of B^{3+} , Fe^{3+} , and Ga^{3+} for Al^{3+} and Ge^{4+} for Si^{4+} , and interlayer cation substitutions of Rb^+ , Cs^+ , NH_4^+ , and Na^+ for K^+ provide additional data on linear relationships that exist between ionic radii (Shannon and Prewitt) and unit cell edges, and between (ionic radii)³ and unit cell volumes of these micas. The influence of substitutions on the unit cell are such that octahedral substitutions predominantly affect the a -dimension, interlayer substitutions the c -dimension, and tetrahedral substitutions affect both dimensions.

Tetrahedral and interlayer cation substitutions of a wide range of ionic radii were found to form stable micas. However, octahedral cations of greater than 0.78 Å average ionic radius do not form stable trioctahedral micas of the form $\text{KR}_3^{2+} \text{AlSi}_3\text{O}_{10} (\text{OH})_2$. The instability of such micas is shown to be due to the misfit of smaller tetrahedral layers onto a larger octahedral layer. The composition of natural biotites are explained on the basis of this model. In addition, quantitative predictions of the amount of Fe^{3+} in octahedral and tetrahedral positions in synthetic annite were made, and have been confirmed by Mössbauer and analytical chemistry techniques. A nomogram is constructed from which, for any given composition of a hydrous trioctahedral mica, the relative stability of the mica may be determined.

INTRODUCTION

Trioctahedral micas are subject to a wide variety of cation substitutions. Several authors have demonstrated that such substitutions have a profound effect on both the physical properties and the stabilities of these layer silicates (Hatch *et al.*, 1957; Wones, 1963b; Klingsberg and Roy, 1957). A list of several recent studies on synthetic hydrous trioctahedral micas is given in Table 1. While data are now available for a dozen such mica end-members, there has been little attempt to systematically examine changes in mica properties with composition. The present study is an attempt to define quantitatively

¹ Present address: U. S. Geological Survey, Washington, D. C. 20242

TABLE 1. Previous Studies of Synthetic Hydrrous Trioctahedral Micas

<u>Composition</u>	<u>Emphases of Study</u>	<u>References</u>
$\text{KMg}_3\text{AlSi}_3\text{O}_{10}(\text{OH})_2$	Physical Properties & Stability Stability Structure	Yoder & Eugster (1954) Wones (1967) Steinfink (1962)
$\text{KFe}_3\text{AlSi}_3\text{O}_{10}(\text{OH})_2$	Stability & Physical Properties Stability & Physical Properties	Eugster & Wones (1962) Wones, Burns & Carroll (1971)
$\text{K}(\text{Mg},\text{Fe})_3\text{AlSi}_3\text{O}_{10}(\text{OH})_2$	Physical Properties Stability	Wones (1963) Wones & Eugster (1965)
$\text{KMg}_3\text{FeSi}_3\text{O}_{10}(\text{OH})_2$	Physical Properties	Wise & Eugster (1964)
$\text{KFe}_3\text{FeSi}_3\text{O}_{10}(\text{OH})_2$	Physical Properties	Wones (1963a)
$\text{KMg}_3\text{BSi}_3\text{O}_{10}(\text{OH})_2$	Physical Properties Physical Properties	Eugster & Wright (1960) Stubicon & Roy (1962)
$\text{KMg}_3\text{GaSi}_3\text{O}_{10}(\text{OH})_2$ $\text{KNi}_3\text{AlSi}_3\text{O}_{10}(\text{OH})_2$	Stabilities only	Klingsberg & Roy (1957) DeVries & Roy (1958)
$\text{KZn}_3\text{AlSi}_3\text{O}_{10}(\text{OH})_2$ $\text{KMn}_3\text{AlSi}_3\text{O}_{10}(\text{OH})_2$	Unit Cell Parameters	Frondel & Ito (1966)
$\text{NaMg}_3\text{AlSi}_3\text{O}_{10}(\text{OH})_2$	Physical Properties	Carman (1969)
$\text{NH}_4\text{Mg}_3\text{AlSi}_3\text{O}_{10}(\text{OH})_2$	Physical Properties	Eugster & Munoz (1966)

the effects of a wide range of cation substitutions on the physical properties of hydrous trioctahedral micas.

MICA COMPOSITIONS STUDIED

The hydrous magnesian trioctahedral mica, phlogopite- $\text{KMg}_3\text{AlSi}_3\text{O}_{10}(\text{OH})_2$, was used as the reference composition in this study. Attempted 100 percent octahedral substitutions for Mg^{2+} included Mn^{2+} , Co^{2+} , Ni^{2+} , Cu^{2+} , Zn^{2+} , Cd^{2+} , and Pb^{2+} . Data of Wones (1963b) on the Fe^{2+} mica annite, and synthetic biotites on the join phlogopite-annite, have also been employed. Tetrahedral cation substitutions were Ga^{3+} , Fe^{3+} , and B^{3+} for Al^{3+} , and Ge^{4+} for Si^{4+} ; while substitutions into the interlayer cation K^+ position include Rb^+ , Cs^+ , Cu^+ , and Ag^+ . In addition, Na^+ phlogopite data of Carman (1969) and NH_4^+ phlogopite data of Eugster and Munoz (1966) have been used in this study. Finally, a number of double 100 percent cation substitutions into the phlogopite structure were studied, including ferriannite- $\text{KFe}_3^{2+}\text{Fe}^{3+}\text{Si}_3\text{O}_{10}(\text{OH})_2$ (data of Wones, 1963a), nickelous ferriphlogopite- $\text{KNi}_3\text{FeSi}_3\text{O}_{10}(\text{OH})_2$, cobaltous ferriphlogopite- $\text{KCo}_3\text{O}_{10}(\text{OH})_2$, and sodium-zinc phlogopite- $\text{NaZn}_3\text{AlSi}_3\text{O}_{10}(\text{OH})_2$.

EXPERIMENTAL TECHNIQUE

A complete list of chemicals and their lot numbers used in starting material preparation will be found in Table 2. Cobaltous hydroxide was prepared by the T. A. Edison precipitation method (U. S. Patent #1,167,484) in which ammonium hydroxide is added to a cobaltous sulfate solution. The precipitate of $\text{Co}(\text{OH})_2$ is washed five times in deionized and distilled water, and then dried at 100°C for 4 h. γ -alumina was prepared by heating $\text{AlCl}_3 \cdot 6\text{H}_2\text{O}$ for 1 h. at 750°C . The silica glass was cleaned both magnetically and in acid, and fired at 800°C for 2 h. before using. $\text{K}_2\text{O} \cdot 2\text{SiO}_2$ was prepared by D. R. Wones from cleaned SiO_2 glass and KHCO_3 after the method of Schairer and Bowen (1955). Starting materials of five types were used:

- 1) Oxide Mix
- 2) $\text{K}_2\text{Si}_2\text{O}_6$ plus oxides
- 3) KAlSi_3O_8 gel plus R^{2+} oxide or hydroxide
- 4) KFeSi_3O_8 gel plus R^{2+} oxide or hydroxide
- 5) Mica gel

All gels were prepared by titration of standardized nitrate solutions. The solution mixes were dried and fired as described by Shaw (1963). Oxide mixes were prepared by weighing and mixing dried oxides or hydroxides, and then grinding in an agate mortar until optically homogeneous.

Charges were sealed with excess and deionized and distilled water, or 30 percent H_2O_2 solution in Au or $\text{Ag}_{90}\text{Pd}_{10}$ $\frac{1}{8}$ in $\times \frac{1}{2}$ in capsules. In several runs oxygen fugacities were controlled by the solid buffer technique of Eugster (1957). Standard cold seal hydrothermal pressure apparatus was used in all runs (Tuttle,

1949). Pressure measurements are believed accurate within 1 per cent, and the error in temperature is within $\pm 3^\circ\text{C}$. All runs were rapidly quenched (2 min.) in a cool water bath. A partial list of synthesis experiments will be found in Table 3.

X-ray powder diffraction examination of all runs was performed on a Picker diffractometer using $\text{Cu K}\alpha$ radiation, and data was collected on a strip chart recorder. Both CaF_2 (Baker's Analytical Reagent lot #91548; annealed 3 times at 800°C for 1 h.; $a = 5.4620 \pm .0005\text{\AA}$) and BaF_2 (Baker's lot #308; annealed 2 times at 800°C for 1 h.; $a = 6.1971 \pm .0002\text{\AA}$) were employed as internal standards. Least squares unit cell refinements were performed using the Evans, Appleman, and Handwerker (1963) program. Optical data were obtained using a Zeiss binocular polarizing microscope with a white light source. Mica indices of refraction were measured with Cargille's Index of Refraction Liquids, which are accurate to within $\pm .0005$. All X-ray diffraction and optical work was performed at room temperature ($24^\circ \pm 1^\circ\text{C}$).

UNIT CELL PARAMETERS

1M unit cell dimensions and volumes, as well as molecular weights and calculated densities, for synthetic hydrous trioctahedral micas of

TABLE 2. Chemicals used in starting material preparation

Chemicals used in oxide mix preparation		
<u>Formulae</u>	<u>Manufacturer (& Grade)*</u>	<u>Lot Number</u>
SiO_2 glass	Corning (lump cullet)	7940
GeO_2 (trigonal)	Fisher	786604
$\text{AlCl}_3 \cdot 6\text{H}_2\text{O}$	Mallinkrodt	15961X
Fe_2O_3	Fisher	762942
B_2O_3	J.T. Baker	39315
MgO	Fisher	787699
MnO	K & K	10868
$\text{CoSO}_4 \cdot 7\text{H}_2\text{O}$	Mallinkrodt	n.d.
NiO	Matheson, Coleman & Bell	CB918 NX345
CuO	Mallinkrodt	X40588
ZnO	Baker & Adamson	B354
CdO	Baker & Adamson	A244X364J
Ni(OH)_2	K & K	16214
$\text{NH}_4\text{(OH)}$	J.T. Baker	24037
KHCO_3	J.T. Baker	21537
K(OH)	J.T. Baker	14890
Ag_2O	K & K	17692
Cu_2O	Fisher	n.d.

TABLE 2. Continued
 Additional chemicals used in gel preparations

<u>Formulae</u>	<u>Manufacturer (& Grade)*</u>	<u>Lot Number</u>
"Ludox" **	Dupont (High Silica)	n.d.
Ag Metal	Fisher	71096
Cu Metal	Baker & Adamson	N-023
Zn Metal	Merck	40678
Pb Metal	Fisher (8/1000" foil)	n.d.
Ga Metal	J.T. Baker (99.999%)	n.d.
KNO ₃	J.T. Baker	30158
NaNO ₃	J.T. Baker	33275
RbNO ₃	K & K	18088
CsNO ₃	K & K	7824
Mg(NO ₃) ₂ ·6H ₂ O	Mallinkrodt	37012
Mn(NO ₃) ₂	Mallinkrodt (50% solution)	27357
Al(NO ₃) ₃ ·9H ₂ O	Mallinkrodt	26829
Cr(NO ₃) ₃ ·9H ₂ O	Mallinkrodt	795204

*All chemicals reagent grade unless noted.

**Dupont Ludox was analyzed by F. Frey. Solids after drying and firing at 300°C include by weight SiO₂ = 99.0% and Na₂O = 1.0%.

this and other studies are listed in Table 4. All parameters were refined using at least twenty equally-weighted X-ray powder reflections, except for Rb⁺ and Cs⁺ micas for which only three broad peaks were observed. Smith and Yoder (1956) have shown that trioctahedral micas often possess an ideal pseudo-trigonal unit cell, defined by $a_m = b_m / (3)^{1/2}$ and $d_{001} = c_m \cdot \sin \beta_m$. Of the micas examined, only sodium and boron phlogopites depart appreciably from these ideal relations.

Crowley and Roy (1960) have demonstrated that pressure of formation does not significantly affect unit cell parameters of phlogopite. Similarly, synthetic micas examined in this study showed no systematic variations of cell parameters with temperature or pressure of crystallization. However, Eugster and Wright (1966) have noted that the physical properties of boron phlogopite appear to vary with temperature and pressure of formation. Also, Carman (1969) has clearly documented the tendency of sodium phlogopite to hydrate below 80°C.

Thus, sodium and boron phlogopite once again depart from the ideal case. It should be noted that sodium and boron phlogopites have the smallest cell dimensions of all micas studied.

OPTICAL DATA

Indices of refraction for synthetic hydrous trioctahedral micas of this and other studies are found in Table 5. Due to the pseudo-trigonal habit of these micas, $\gamma \approx \beta$, and thus two refractive indices are definitive. Other optical parameters considered include birefringence $B = \gamma - \alpha$ and the observed mean refractive index $\bar{n} = \sqrt[3]{\alpha \cdot \gamma^2} \approx (2\gamma + \alpha)/3$. While synthetic crystallites seldom exceeded 20μ in size, thus making

TABLE 3. Mica Synthesis Experiments

Substituting cation	Ionic ¹ radius (Å)	Run #	2. Duration		Starting Materials	Products
			T (°C±1°)	(hours)		
Micas of the form $R^+Mg_3AlSi_3O_{10}(OH)_2$						
K ⁺	1.38	M#1	800	70	gel	100% phlogopite
Rb ⁺	1.49	M#105	700	140	gel	Rb-phlogopite, Forsterite, & RbAlSi ₂ O ₆
		M#98	300	340	gel	do. plus glass
Cs ⁺	1.70	M#106	700	140	gel	Cs-Phlogopite, Forsterite, & CsAlSi ₂ O ₆
		M#99	300	340	gel	Forsterite, CsAlSi ₂ O ₆ & glass
Ag ⁺	1.15	M#46	310	48	gel	Silver Metal & glass
		M#90	600	72	MgAlSi ₃ gel plus Ag ₂ O	Silver Metal, Chlorite & glass
Cu ⁺	0.96	M#122	630	96	Oxide Mix	Cu ₂ O, Talc & unknown phase
Micas of the form $KR_3^{+2}AlSi_3O_{10}(OH)_2$						
Mg ⁺²	0.720	M#1	800	70	gel	100% Phlogopite
Mn ⁺²	0.83	M#13	450	96	Oxide Mix & K ₂ Si ₂ O ₅ gel	α -Mn ₂ O ₃ ; γ -Mn ₂ O ₃ & sanadine
		M#18	280	216	Reduced Oxide Mix	MnO; Mn(OH) ₂ & glass
		M#19	326	120	"	Tephroite, Kalsilite & Leucite
		M#32	603	120	gel	Mn(OH) ₂ & Manganophyllite
		M#62	725	72	"	γ -Mn ₂ O ₃ & Sanidine
		M#86	540	96	Reduced gel	Braunite & Sanidine
Micas of the form $KR_3^{+2}AlSi_3O_{10}(OH)_2$						
Co ⁺²	0.745	M#91 ³	500	336	M#32	Mn(OH) ₂ & Manganophyllite
		M#92 ³	500	336	gel	Tephroite, Kalsilite & Leucite
		M#117 ³	600	96	MnO plus Rfs gel	Tephroite, Kalsilite & Leucite
		M#114	750	48	Co(OH) ₂ + gel	100% Cobaltous phlogopite
Ni ⁺²	0.69	SR#12	710	48	Co(OH) ₂ + gel	100% Cobaltous phlogopite
		SR#34 ⁴	880	48	SR#12	CoO, Co Olivine & Leucite
		M#76	600	145	Oxide Mix + K ₂ Si ₂ O ₅ gel	100% Nickelous Phlogopite
Cu ⁺²	0.73	M#15	750	48	Ni(OH) ₂ + gel	100% Nickelous Phlogopite
		M#29	600	120	gel	80% Cupric Phlogopite, glass and minor unidentified phase
		M#49	703	96	gel	50% Cupric Phlogopite, glass and unidentified phase
Zn ⁺²	0.75	M#77	260	215	gel	Cupric Phlogopite, Cu-Pyroxene & Muscovite
		M#8	600	145	Oxide mix & K ₂ Si ₂ O ₅	Willemite, Kalsilite, & Leucite
		M#17	280	215	Oxide mix & K ₂ Si ₂ O ₅	Willemite, Mica & minor Leucite

1. Shannon and Prewitt (1970).
2. All runs at P = 2 kbar H₂O unless noted.
3. P = 1.0 kbar CH₄.
4. P = 0.2 kbar H₂O.

Substituting cation	Ionic radius (Å ^e)	Run #	T (°C±3°)	Duration (hours)	Starting Materials	Products
Cd ⁺²	0.95	M#61	725	72	gel	Willemite, Kalsilite & Leucite
		M#94	530	50	gel	Willemite, Mica & Leucite
		M#101	500	290	gel	Willemite, Mica & Leucite
		M#9	600	145	Oxide mix & K ₂ Si ₂ O ₅	Cd-Olivine & Leucite
		M#22	385	360	Reduced Oxide mix	Cd-Olivine & Sanidine
Pb ⁺²	1.18	M#57	650	290	gel	Pb ₄ SiO ₆ & unknown phase
		M#66	410	170	gel	K ₂ Pb ₄ Si ₈ O ₂₁ , Sanidine & Pb ₃ O ₄
Al ⁺³ B ⁺³	0.39 0.12	Micas of the form KMg ₃ R ⁺³ Si ₃ O ₁₀ (OH) ₂				
		M#1	800	70	gel	100% Phlogopite
Ga ⁺³	0.47	M#30	603	120	Oxide Mix & K ₂ Si ₂ O ₅	50% Boron Phlogopite, glass
		M#108	720	120	Oxide Mix & K ₂ Si ₂ O ₅	95% Boron Phlogopite
Fe ⁺³	0.49	M#46	310	45	gel	40% Gallium Phlogopite, Ga ₂ O ₃ , unknown phase & glass
		M#109	720	120	gel	100% Gallium Phlogopite
Cr ⁺³ (IV)	n.d.	M#100	500	265	Oxide Mix & K ₂ Si ₂ O ₅	100% Ferri-Phlogopite
		M#107	720	120	Oxide Mix & K ₂ Si ₂ O ₅	100% Ferri-Phlogopite
		M#111	690	215	Oxide Mix & K ₂ Si ₂ O ₅	100% Ferri-Phlogopite
Si ⁺⁴ Ge ⁺⁴	0.26 0.40	Micas of the form KMg ₃ AlR ₃ ⁺⁴ O ₁₀ (OH) ₂				
		M#44	700	96	gel	Cr ₂ O ₃ , Forsterite & unknown phase
Mg ⁺²	0.72	M#72	410	31	gel	Cr ₂ O ₃ , Forsterite & glass
		M#1	800	70	gel	100% Phlogopite
Ni ⁺²	0.69	M#63	725	75	Oxide Mix	100% Ga-Phlogopite
		Micas of the form KR ₃ ⁺² FeSi ₃ O ₁₀ (OH) ₂				
Co ⁺²	0.745	M#100	500	265	Oxide Mix & K ₂ Si ₂ O ₅	100% Ferri-Phlogopite
		M#107	720	120	Oxide Mix & K ₂ Si ₂ O ₅	100% Ferri-Phlogopite
		M#111	690	215	Oxide Mix & K ₂ Si ₂ O ₅	100% Ferri-Phlogopite
Ni ⁺²	0.69	M#123	700	24	Ni(OH) ₂ & KFeSi ₃ O ₈	100% Nickelous Ferri-Phlogopite
		M#127	700	24	Co(OH) ₂ & KFeSi ₃ O ₈	100% Cobaltous Ferri-Phlogopite

2V determination difficult, all observed 2V ≈ 0°. Micas are colorless except for those containing cations of the transition metal series. Intense pleochroism was observed only in iron-bearing trioctahedral micas, whereas faint pleochroism was noted in cobalt and copper phlogopites.

A useful, but seldom used, optical property is the specific refractive energy *K*, defined by $K = \bar{n} - 1/\rho$ where \bar{n} is the mean refractive index and ρ the density. Gladstone and Dale (1864) demonstrated that *K* for liquids may be calculated from the formula: $K = k_1(P_1/100) + k_2(P_2/100) + \text{etc.}$, where $k_1, k_2, \text{etc.}$ are the specific refractive energies of the components of the liquids and $P_1, P_2, \text{etc.}$ are the weight percentages of these components. H. W. Jaffe (1956) applied the rule of Gladstone and Dale to minerals, treating oxides as components of the minerals. Jaffe obtained reasonable agreement between observed and

TABLE 4. Unit Cell Parameters of Synthetic Hydrous Trioctahedral Micas

Composition	Micas of Known Composition										Run# or Reference
	a_m (Å°)	b_m (Å°)	c_m (Å°)	β_m	V_{01} (Å°) ³	GFW	ρ_{calc} gm/cm ³				
$\text{KMg}_3\text{AlSi}_3\text{O}_{10}(\text{OH})_2$	5.315±.001	9.204±.002	10.311±.003	99°54'±4'	497.0±0.6	417.3	2.79	M#1			
	5.314±.001	9.208±.002	10.314±.005	99°54'±2'	497.0±1.0			Wones (1966)			
	5.314±.01	9.204±.02	10.314±.005	99°54'±5'	497.0±1.0			Yoder & Eugster (1954)			
$\text{Na}^+\text{Mg}_3\text{AlSi}_3\text{O}_{10}(\text{OH})_2$	5.265±.008	9.203±.006	9.994±.001	97°45'±8	479.8±0.8	401.2	2.78	Carman (1969) 1			
NH_4^+	5.311±.008	9.224±.004	10.443±.007	99°42'	504.2	396.2	2.61	Eugster & Muroz (1966)			
Rb^+	5.34 ±.01	9.24 ±.02	10.48 ±.05	99°54'	510.0	463.6	3.02	M#105 2			
Cs^+	5.37 ±.01	9.30 ±.02	10.83 ±.05	99°54'	516.8	510.8	3.18	M#106 2			
$\text{KCO}_3^+\text{AlSi}_3\text{O}_{10}(\text{OH})_2$	5.340±.001	9.240±.005	10.345±.002	99°58'±2	502.8±0.3	521.1	3.44	M#114			
	5.341±.001	9.240±.002	10.347±.002	99°54'	503.3			SR#12 2			
Ni_3^{+2}	5.303±.005	9.172±.001	10.286±.002	99°56'±3'	493.1±.5			M#7b			
Ni_3	5.297±.003	9.175±.003	10.281±.004	99°50'±3'	492.3±.3	520.5	3.51	M#115			
	n.d.	n.d.	10.17	n.d.	n.d.			Klingsberg & Roy (1957)			
Cu^{+2}	5.334±.001	9.238±.002	10.314±.004	99°54'	498.8±.4	535.0	3.56	M#29 2			
Cu_3^{+2}	5.330±.001	9.234±.002	10.316±.003	99°56'±2'	497.8±.2			M#49			
Fe^{+2}	5.401±.01	9.347±.005	10.297±.01	100°10'±12'	511.7	511.9	3.32	Wones (1963b)			
Fe_3	5.397±.001	9.348±.002	10.316±.005	99°54'±	512.0			Wones, Burns & Carrol (1971)			
$(\text{FeMg})_3$ Mole % Fe	5.339±.006	9.230±.001	10.311±.002	99°50'±4'	500.6			Wones (1963b)			
0.169	5.333±.002	9.242±.001	10.312±.001	99°56'±1'	500.6			Wones, Burns & Carrol (1971)			
0.352	5.349±.005	9.260±.002	10.293±.006	99°38'±6'	502.6			Wones (1963b)			
0.450	5.343±.007	9.276±.001	10.312±.003	99°57'±4'	503.4			Wones (1963b)			
0.550	5.358±.003	9.285±.003	10.297±.002	100°0'±1'	504.5			Wones, Burns & Carrol (1971)			
0.765	5.373±.01	9.312±.003	10.297±.009	100°3'±6'	507.3			Wones (1963b)			
0.880	5.389±.003	9.335±.002	10.322±.004	99°58'±4'	511.4			Wones (1963b)			

TABLE 4. Continued

Composition	a_m (Å ²)	b_m (Å ²)	c_m (Å ²)	β_m	Vol. (Å ³)	GFV	Peak 3 gm/cm	Run # or Reference ^a
$KMg_3B^+Si_3O_{10}(OH)_2$	5.29±.02	9.177±.001	10.246±.002	98°34'±4'	491.9±.2	401.1	2.77	M#108
	5.32±.01	9.165±.02	10.29 ±.01	100°10'±10'	496.5			Eugster & Wright (1960)
	5.310	9.150	10.234	100° 8'	489.5			Stubicon & Roy (1962)
Ga^+3	5.327±.002	9.218±.005	10.359±.002	99°49'±2'	501.2±.3	460.0	3.05	M#109
	n.d.	n.d.	10.26	n.d.	n.d.			Klingsberg & Roy (1957)
Fe^+3	5.354±.001	9.273±.002	10.316±.004	99°54'	505.0±.2	446.1	2.93	M#107 2
	5.358±.003	9.276±.003	10.321±.004	99°58'±4'	505.2±.3			M#111 3
	5.34 ±.01	9.28 ±.005	10.35 ±.01	99°55'±10'	505.6			Wise & Eugster (1964)
$KMg_3Al^{+2}O_{10}(OH)_2$	5.393±.002	9.341±.004	10.600±.002	99°54'	526.1±1.0	550.8	3.48	M#63 2
	5.387±.002	9.378±.02	10.593±.003	99°43'±2'	525.5±1.0	550.8		M#68
$KFe^+2Fe^+3Si_3O_{10}(OH)_2$	5.430±.002	9.404±.005	10.341±.006	100°4'±10'	519.9	540.76	3.45	Wones (1963a)
$KMg_3Fe^+3Si_3O_{10}(OH)_2$	5.335±.005	9.237±.005	10.332±.006	99°55'±10'	501.5±.08	549.34	3.63	M#123
$KCo_3Fe^+3Si_3O_{10}(OH)_2$	5.368±.001	9.329±.002	10.346±.002	99°50'±5'	510.1±.04	550.00	3.58	M#127

Synthetic Miccas of Unknown Composition

R^{+2} Cation & Extra Phases								
Zn ⁺²	5.31±.02	9.205±.01	10.25±.05	99°50'±10'	492.5±1.0			M#17
Willemite 25% in all runs	5.303±.004	9.214±.005	10.285±.003	99°41'±3'	495.4±.4			M#94
	5.328±.002	9.226±.002	10.312±.004	99°59'±1'	498.9±.2			M#101
Willemite reported from all runs	5.325±.005	9.210±.005	10.210	99°50'±10'	493.0±1.0			Frondel & Ito (1966)
Mn ⁺²	5.27±.01	9.20±.02	10.17±.03	99°50'±10'				M#32
Mn(OH) ₂ 25% in all runs	5.31±.01	9.21±.01	10.31±.01	99°45'±6'	503±3			M#91
Tephroite reported in all runs	5.32±.01	9.394±.01	10.32±.01	99°50'±10'				Frondel & Ito (1966)

1. X-ray diffraction performed at 130°C.
 2. LM unit cell calculated from ideal 3T cell data.
 $a_m = a$, $b_m = \sqrt{3}a$, $c_m = ct/3 \sin 99°54'$, $\beta_m = 99°54'$
 3. Mössbauer analyses of ferrillopopites by R. Burns reveals 5 to 15% Fe⁺² in all runs.
 4. Unit cell parameters calculated on the Appelman, Handwerker & Evans Program by this author from Frondel & Ito (1966), Table 7, p. 1421.

TABLE 5. Optical Properties of Synthetic Hydrrous Tricoctahedral Micas

Composition	$\bar{\mu}$	\bar{Y}	$\frac{B}{\bar{\mu}}$	$\frac{1}{\bar{\mu}_{obs}}$	$\frac{2}{\bar{\mu}_{calc}}$	Deviation $\frac{\Delta \bar{\mu}}{\bar{\mu}}$	Color, pleochroism & other remarks	Pun# or Reference
$KMg_3AlSi_3O_{10}(OH)_2$	1.550 .002	1.587 .002	0.037	1.575	1.586	+0.011	Colorless, 2V=0°	M#1
Na ⁺	1.550 .002	1.581 .001	0.031	1.571			"	Wones (1966)
Rb ⁺	1.548 .003	1.588 .003	0.040	1.575		+0.011	"	Yoder & Eugster (1954)
Cs ⁺	1.545 .003	1.569 .004	0.024	1.561	1.581	+0.020	Colorless	Carman (1969) ⁴
	1.540 .01	1.575 .01	0.035	1.560	1.647	+0.087	Colorless	M#105
	1.570 .01	1.605 .01	0.035	1.590	1.601	+0.011	Colorless	M#106
Fe ⁺²	1.633 .002	1.700 .002	0.067	1.678	1.667	-0.011	Pleochroic: X = Red or Yellow-brown Z = light green	Wones (1963b)
	1.636 .002	1.690 .002	0.055	1.672		-0.005		Wones & Carroll (1971) ⁵
Co ⁺²	1.607 .002	1.668 .002	0.061	1.648	1.688	+0.040	Pale Purple to Lavender	M#114
Ni ⁺²	1.614 .002	1.675 .002	0.061	1.654	1.702	+0.048	Medium green 2V=0°	M#115
	n.d.	1.652						Klingsberg & Roy (1957)
Cu ⁺²	1.588 .004	1.630 .004	0.042	1.616	1.690	+0.074	Medium blue	M#29
	1.549 .002	1.580 .002	0.031	1.570	1.581	+0.011	Colorless	M#108
	1.546 .002	1.568 .002	0.022	1.560		+0.021	"	Eugster & Wright (1960)
Ga ⁺³	1.558 .003	1.598 .003	0.040	1.585	n.d.	n.d.	Colorless	M#109
	n.d.	1.598						Klingsberg & Roy (1957)
Fe ⁺³	1.601 .002	1.642 .002	0.041	1.628	1.656	+0.028	Pleochroic: X = reddish-brown Z = pale orange	M#111
	1.600 .001	1.642 .001	0.040	1.629		+0.027		Wise & Eugster (1964)
Ge ⁺⁴	1.596 .003	1.646 .003	0.050	1.623	n.d.	n.d.	Colorless	M#63
Fe ⁺² Fe ⁺³	1.705 .005	1.748 .003	0.043	1.734	1.711	-0.023	n.d.	Wones (1963a)
Co ⁺² Fe ⁺³	1.715 .005	1.760 .005	0.0	1.745	1.787	+0.042	x=red-brown z= pale purple	M#127
Ni ⁺² Fe ⁺³	1.730 .005	1.770 .005	0.040	1.757	1.799	+0.042	x=red-brown z=pale green	M#123

1. $B = \bar{\mu} - \bar{\alpha}$ 2. $\bar{n} = \sqrt{\frac{\bar{\mu} + \bar{\alpha}}{\bar{\mu} - \bar{\alpha}}} = \sqrt{\frac{\bar{\mu} + 2\bar{\alpha}}{\bar{\mu} - \bar{\alpha}}}$ 3. $\bar{\mu}_{calc.} = \rho \cdot k + 1$, where ρ = density in gm/cm³ and k = specific refractive energy after the rule of Gladstone and Dale (1864).

4. Indices of refraction determined on micas heated to 80°C and immediately placed into oil.

5. Recent Mossbauer work reveals appreciable Fe⁺³ in all synthetic annites.

calculated \bar{n} in this manner. However, it is interesting to note that the calculated \bar{n} for hydrous silicates considered in Jaffe's study displayed consistent positive deviations from observed \bar{n} . Deviations ranged from a low of -0.001 to as high as $+0.064$ for the twenty-five hydrous-silicates discussed.

Similarly, synthetic hydrous micas of this study display consistently positive deviations of $\bar{n}_{\text{calc.}}$ from $\bar{n}_{\text{obs.}}$. Only annites display a negative deviation, and positive deviations as high as $+0.087$ are noted. It would thus appear that the value cited for $k(\text{H}_2\text{O})$ by Larsen and Berman (1934) of 0.034 cannot be applied directly to water in the silicate minerals. A significantly smaller value for $k(\text{H}_2\text{O})$ is implied by the above data. Another source of error in the calculated K for silicates may result from erroneous k values for transition metals. Jaffe (1956) notes that $k(\text{Fe}_2\text{O}_3)$ varies from 0.290 in silicates to 0.404 in oxides. It thus appears that k for transition metals may be lowered considerably in a silicate environment. However, k values for copper, cobalt, nickel, etc. are known only for the oxide environment. This may, in part, explain the anomalously high values for \bar{n} calculated. It seems that further refinement of k values are needed before the rule of Gladstone and Dale may be effectively applied to silicate minerals.

SOURCES OF ERROR

Optical examination revealed that the majority of trioctahedral micas synthesized represent 99+ percent reaction from starting materials, and are thus assumed to be of ideal composition. However, rubidium and cesium phlogopites represented only ≈ 20 –25 percent of the reactants in those runs. These micas are thought to approximate ideal composition on the basis of the observed trioctahedral X-ray patterns and the predicted unit cell parameters. Due to difficulties in standardizing gallium in nitrate solution, the gallium phlogopite gel may be slightly deficient in Ga^{3+} , explaining why a maximum reaction of only 95 percent was obtained. Another possible source of error in the assumed compositions was revealed through Mössbauer studies of iron-bearing phlogopites. Wones, Burns, and Carroll (1971) have shown a minimum of 10 percent Fe^{3+} in all annites, and from 5 to 15 percent Fe^{2+} in ferriphlogopites. Thus, one might also expect multiple valence states in Ni, Co, and Cu-bearing micas. Seifert and Schreyer (1971) have demonstrated the presence of Mg^{2+} in tetrahedral coordination in Mg-rich synthetic trioctahedral micas. However, the assumption is made that all R^{2+} -cations in this study are in octahedral coordination unless noted otherwise.

In the investigation by Frondel and Ito (1966), and in this study,

end-member zinc phlogopite $\text{KZn}_3\text{AlSi}_3\text{O}_{10}(\text{OH})_2$ was not achieved. In all experiments in which mica was produced, ≥ 25 percent willemite- Zn_2SiO_4 with minor leucite and/or glass were also present. While the mica is clearly zinc-bearing, having cell parameters and indices of refraction higher than phlogopite, the excess willemite is evidence of less than three Zn^{2+} atoms per mica formula unit. Neumann (1949) has documented the great preference of zinc for tetrahedral coordination. Thus, one possible explanation for such a zinc-poor mica is that the zinc enters the tetrahedral layer, while aluminum fills the three octahedral sites; *i.e.*, $\text{KAl}_3^{3+}(\text{Zn}_2^{2+}, \text{Si}_2^{4+})_3\text{O}_{10}(\text{OH})_2$. A structural study of the natural zinc mica hendricksite from Franklin, New Jersey, would aid in an understanding of zinc's role in the layer silicates.

Synthesis of end-member manganese phlogopite- $\text{KMn}_3\text{AlSi}_3\text{O}_{10}(\text{OH})_2$ was also unsuccessful. Frondel and Ito (1966) report that tephroite- Mn_2SiO_4 is present as a major phase in all mica-bearing runs, while in the present study pyrochroite- $\text{Mn}(\text{OH})_2$ accompanies the mica phase. Thus, while the unit cell parameters of the mica are greater than those of phlogopite, there are fewer than three manganese atoms per mica formula unit. Burns (1970, p. 43) has demonstrated from absorption spectra evidence that the distorted octahedral site of the phlogopite structure may stabilize manganese in the plus-three valence state. Furthermore, natural manganophyllites invariably contain aluminum in more than 10 percent of the octahedral sites. Therefore, the manganese-poor mica synthesized in this study may represent a solid solution between the components $\text{KMn}_3^{2+}\text{AlSi}_3\text{O}_{10}(\text{OH})_2 + \text{KMn}_2^{3+}\text{AlSi}_3\text{O}_{10}(\text{OH})_2 + \text{KAl}_2\text{AlSi}_3\text{O}_{10}(\text{OH})_2$. Further study on natural manganophyllites is needed to define the extent of $\text{Mn}^{3+}/\text{Mn}^{2+}$ substitution in the mica's distorted octahedral sites.

RELATIONS BETWEEN CELL PARAMETERS AND IONIC RADII

There exist several systematic relations between unit cell parameters and ionic radii of substituting cations. For example, the cell dimensions a_m , b_m , and c_m are each proportional to the Shannon and Prewitt (revised 1970) ionic radii of cations substituting into the tetrahedral, octahedral or interlayer positions. This relation is clearly demonstrated by Figure 1 of b_m vs. octahedral cation radii. The single exception to this rule is that of c_m vs. interlayer six-coordinated cation radii (Fig. 2). The distinct negative curvature has been explained by Prewitt (personal communication) as the result of increasing effective coordination number of the interlayer cation with increasing ionic radius of this cation. For a given cation, an increase in coordination number is accompanied by an increase in effective ionic radius. Assuming the

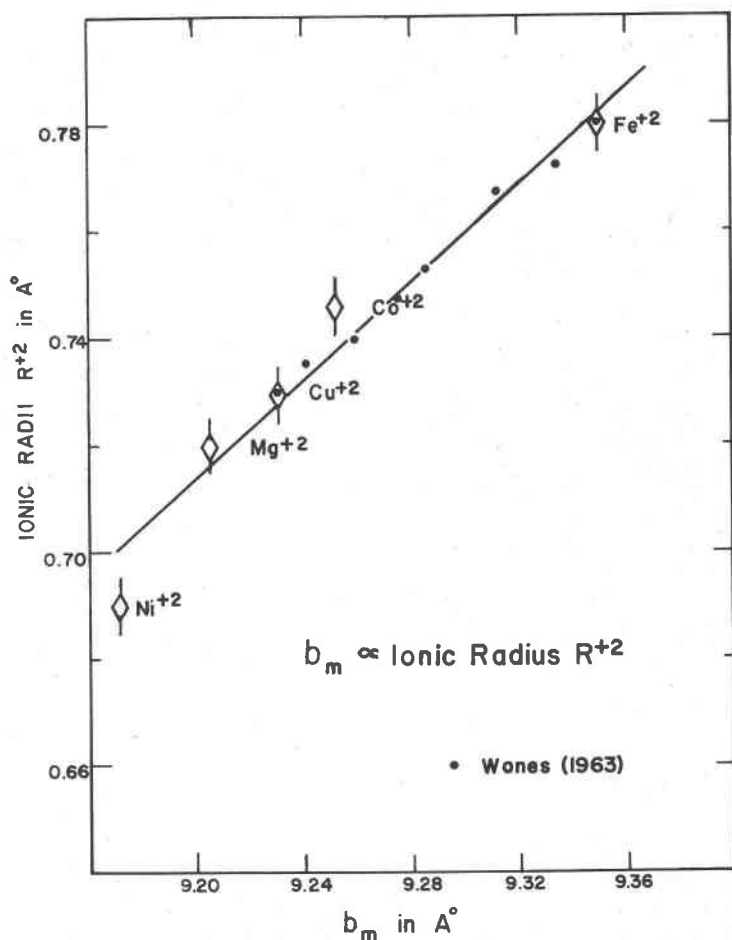


FIG. 1. Monoclinic b_m unit cell dimension vs. ionic radius of the octahedral R^{2+} cation for micas of the form $KR_3^{2+}AlSi_3O_{10}(OH)_2$. Black dots represent biotites on the join phlogopite—annite synthesized by Wones (1963b).

relation C_m vs. effective interlayer cation radius is linear, then the relation C_m vs. six-coordinated cation radius should demonstrate the observed negative curvature. As expected, unit cell volumes are linearly related to the cube of the substituting cations' radii for octahedral and tetrahedral substitutions, and display a slight negative curvature in the interlayer case (Figs. 3 and 4).

It is of interest to consider how b_m (the cell dimension within the mica layers) varies with respect to d_{001} (the dimension perpendicular to the layers) for each type of cation substitution. A plot of b_m vs.

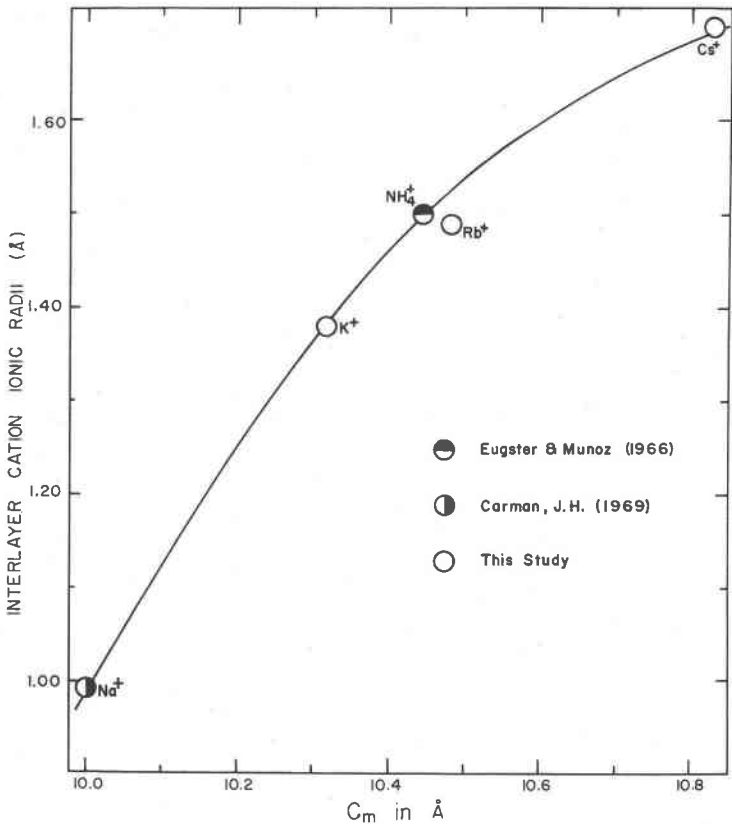


Fig. 2. Monoclinic c_m unit cell dimension vs. ionic radius of the interlayer R^+ cation for micas of the form $R^+\text{Mg}_3\text{AlSi}_3\text{O}_{10}(\text{OH})_2$.

d_{001} (Fig. 5) demonstrates that octahedral, tetrahedral, and interlayer cation substitutions have differing effects on the size and shape of the unit cell. For example, octahedral substitutions have a profound influence on b_m , while d_{001} remains virtually constant. The near-vertical slope of the R^{2+} line is a result of this fact. It should be noted that these observations agree with the theoretical predictions of Takeda and Morimoto (1970). On the other hand, interlayer cation substitutions alter the thickness, d_{001} , of the layers, while having a much smaller effect on b_m . R^{3+} and R^{4+} tetrahedral substitutions influence both b_m and d_{001} .

SUBSTITUTIONS AND STABILITY

Interlayer and tetrahedral cation substitutions demonstrate that a wide range of ionic radii are possible in these positions. Interlayer

cations vary from sodium (ionic radius = 0.98 Å) to cesium (1.70). Tetrahedral cations from boron (0.12) to trivalent iron (0.49) form stable micas. However, octahedral cations seem far more restricted in their ability to substitute into the phlogopite structure. No R^{2+} cation of radius greater than ferrous iron (0.78), including lead (1.18) cadmium (0.95) and manganese (0.83), was found to form a stable mica. Furthermore, Eugster and Wones (1962) have demonstrated that the Fe^{2+} mica, annite, is far less stable than phlogopite. Thus, it appears that the stability of trioctahedral micas may be in part a function of the octahedral cation's radius.

It is well known that in phlogopite the ideal $AlSi_3$ tetrahedral layer is larger than the Mg_3 layer (Radoslovich and Norrish, 1962). If the trioctahedral mica is to be stable, then these two layers must coincide, either by expansion of the octahedral layer in the plane of a_m and b_m or by contraction of the tetrahedral layer within this plane. Radoslovich and Norrish suggest four ways to accomplish this:

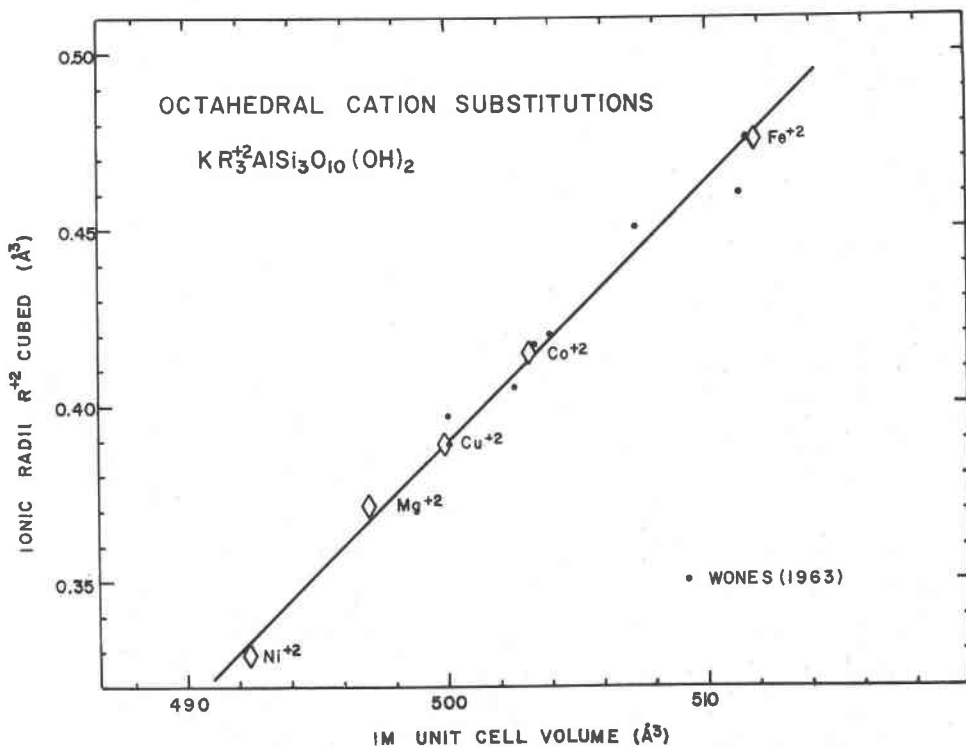


FIG. 3. Monoclinic unit cell volume vs. the cube of the octahedral R^{2+} cation radius for micas of the form $KR_3^+AlSi_3O_{10}(OH)_2$.

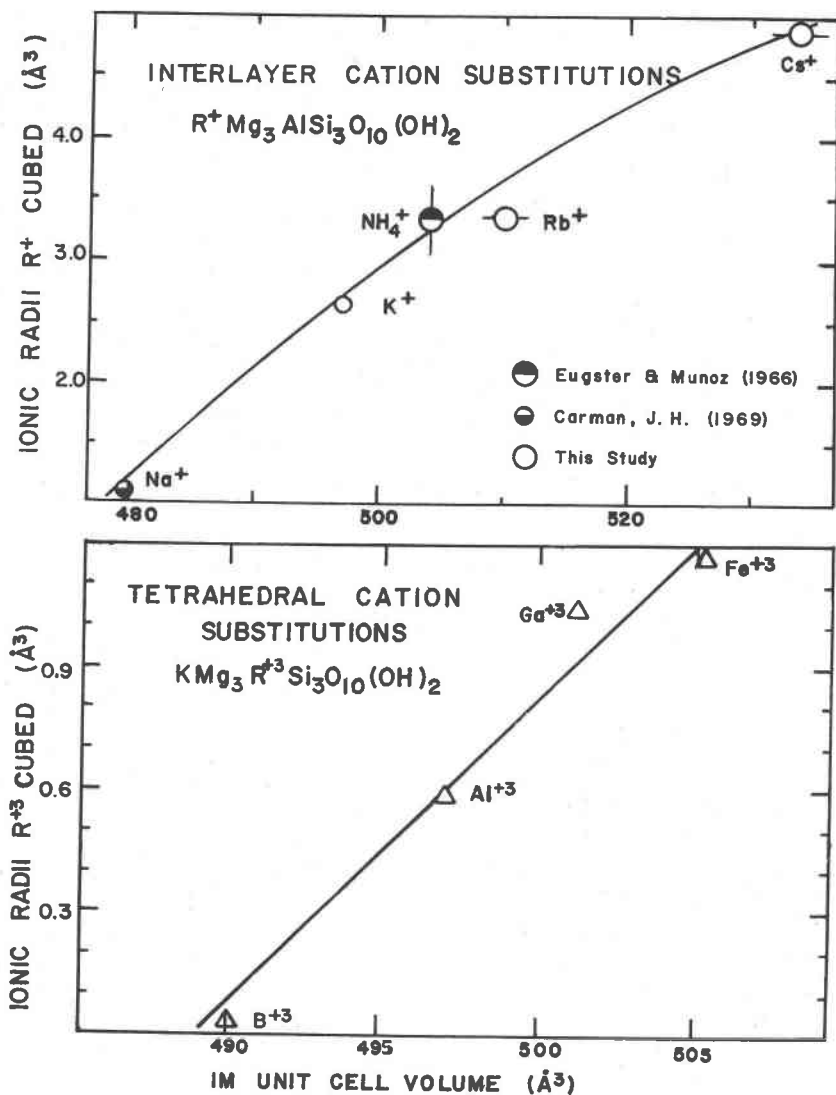


Fig. 4. Monoclinic unit cell volume vs. the cube of the interlayer R^+ cation radius for micas of the form $R^+Mg_3AlSi_3O_{10}(OH)_2$, and vs. the cube of the tetrahedral R^{3+} cation radius for micas of the form $KMg_3R^{3+}Si_3O_{10}(OH)_2$.

- 1) altering bond lengths of the ideal layers,
- 2) tetrahedral layer tilting or corrugation,
- 3) octahedral layer flattening, or
- 4) tetrahedral layer rotation.

The altering of bond lengths is energetically far more difficult than altering bond angles. Thus, while such distortions have been noted in pure fluoropolyolithionite $KAlLi_2Si_4O_{10}F_2$ (Takeda and Burnham, 1969), bond stretching or contraction is assumed to be a minor effect in $AlSi_3$ or $Fe^{3+}Si_3$ tetrahedra. Tetrahedral tilting or corrugation is also well documented by Takeda and Burnham in their mica with partially ordered $AlLi_2$ octahedral layer. However, they believe that tilting of tetrahedra will be minimized when all octahedral positions are filled by the same cation.

Donnay, Donnay, and Takeda (1964) have demonstrated that the

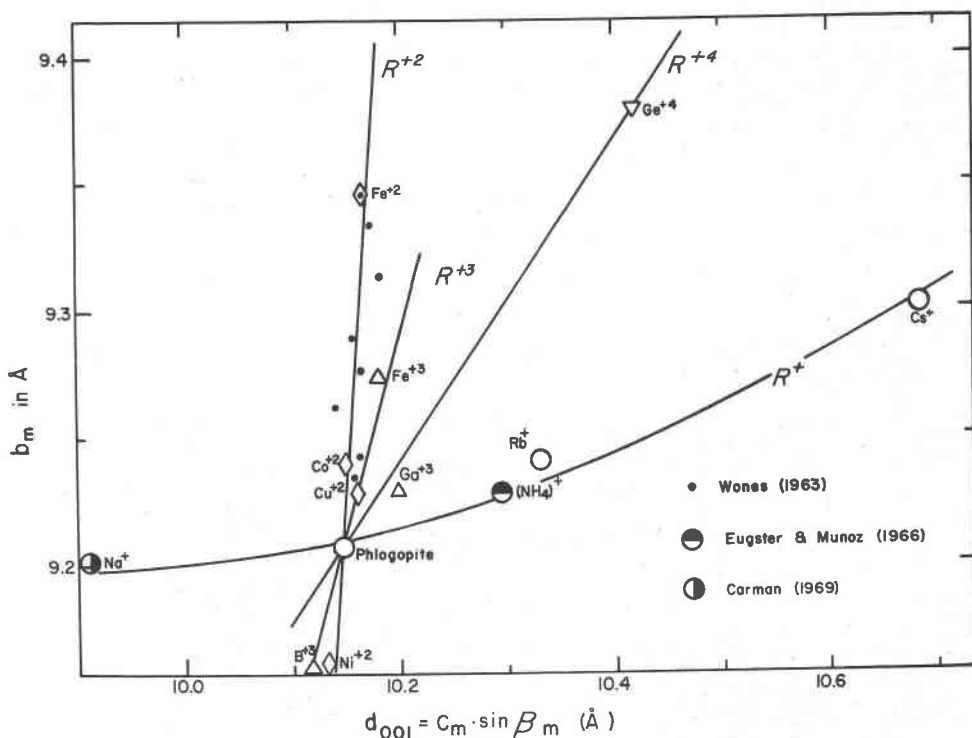


FIG. 5. Monoclinic interlayer spacing d_{001} vs. monoclinic b_m unit cell dimension. The four lines represent micas of the forms $R^+Mg_3AlSi_3O_{10}(OH)_2$, $KR_3^{2+}AlSi_3O_{10}(OH)_2$, $KMg_3R^{3+}Si_3(OH)_2$, and $KMg_3AlR_3^{4+}O_{10}(OH)_2$.

octahedral layer may conform to the larger tetrahedral layer by octahedral layer flattening (See Fig. 6). In this way bond lengths are preserved while bond angles are altered. The amount of compression may be represented by the angle ψ , which has the value $54^\circ 44'$ in an ideal octahedron. If the assumptions are made that:

- 1) there is no tetrahedral tilting or corrugation (*i.e.*, basal oxygens in each tetrahedral sheet are coplanar),
- 2) (001) projections of tetrahedra are equilateral triangles, and
- 3) $a_m = b_m / (3)^{1/2}$,

then ψ is a simple function of the mean octahedral bond length d_o and cell dimension b_m : $\sin \psi = b_m / 3(3)^{1/2} \cdot d_o$. The mean octahedral bond length for Mg—(O, OH) and Fe²⁺—(O, OH) and Fe²⁺—(O, OH) are given by Donnay, Donnay, and Takeda (1964) as 2.07 Å and 2.12 Å respectively. Mean bond lengths for other octahedral cations may be calculated by interpolation or by adding cation radius to that of

OCTAHEDRAL LAYER COMPRESSION

$$\psi = \text{Arc sin } (b_m / 3\sqrt{3} \cdot d_o)$$

$$b_m = 3 \cdot \overline{AB}$$

$$d_o = \overline{MO}$$

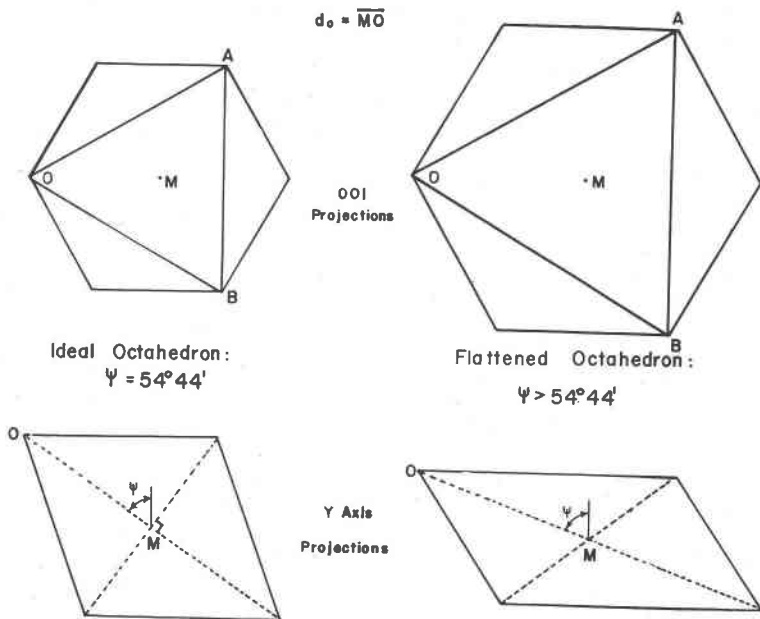


FIG. 6. Expansion of the octahedral 001 projection by octahedral layer compression.

oxygen (1.38 Å). Thus, knowing b_m , we can calculate ψ for each octahedral layer substitution. In Figure 7, ψ is plotted vs. octahedral cation radius. As ionic radius increases, the value of ψ is noted to decrease slightly. Thus, larger octahedral cations require less site flattening to conform to the $AlSi_3$ tetrahedral layer. While octahedral layer flattening is a real effect in hydrous trioctahedral micas, this structural parameter does not explain the instability of 100 percent octahedral substitutions of cations larger than Fe^{2+} .

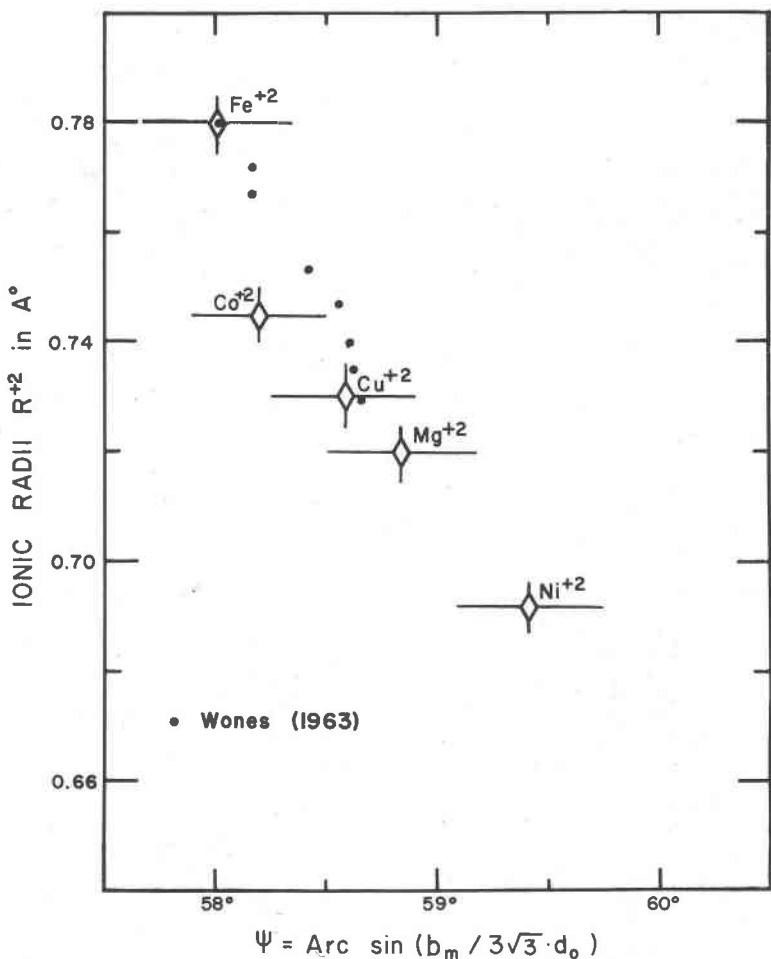


FIG. 7. Octahedral layer compression angle ψ vs. ionic radius of the octahedral R^{2+} cation in micas of the form $KR_3^{2+}AlSi_3O_{10}(OH)_2$. Black dots represent biotites on the join phlogopite-annite synthesized by Wones (1963).

Tetrahedral layer rotation is a fourth means of fitting the non-equivalent octahedral and tetrahedral layers (see Fig. 8). Donnay, Donnay, and Takeda (1964) have shown that by rotating each tetrahedron through an angle α about an axis perpendicular to the (001) plane, the effective size of the tetrahedral sheet is reduced. Structure studies by Steinfink (1962) and others reveal values for α may be greater than 10° in natural micas. Thus, in phlogopite the strain between octahedral and tetrahedral layers may be released primarily through tetrahedral layer rotation.

If the conditions assumed by Donnay, Donnay, and Takeda (1964) for octahedral layer flattening are correct, then α is defined by the mean tetrahedral bond length d_t and the cell dimension b_m : $\cos \alpha = b_m/4 \cdot (2)^{1/2} \cdot d_t$. The mean tetrahedral bond length for the AlSi_3 layer is known to be $1.643 \pm .002 \text{ \AA}$ from studies of muscovite (Güven, 1967 and Burnham and Radoslovich, 1964), biotite (Franzini, 1963), and fluorphlogopite (McCauley, 1968). With this value of d_t , and the

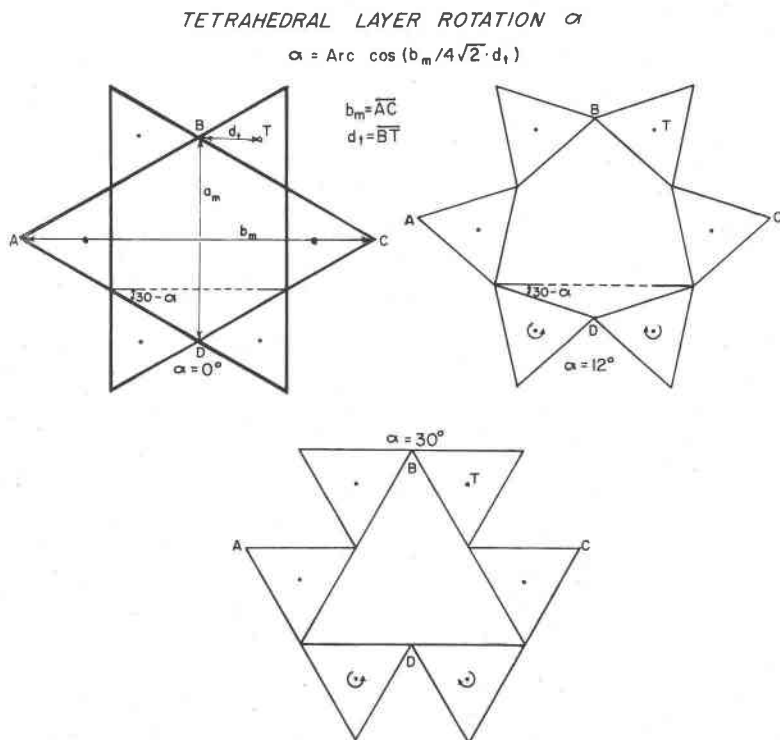


FIG. 8. Contraction of the tetrahedral 001 projection by tetrahedral layer rotation.

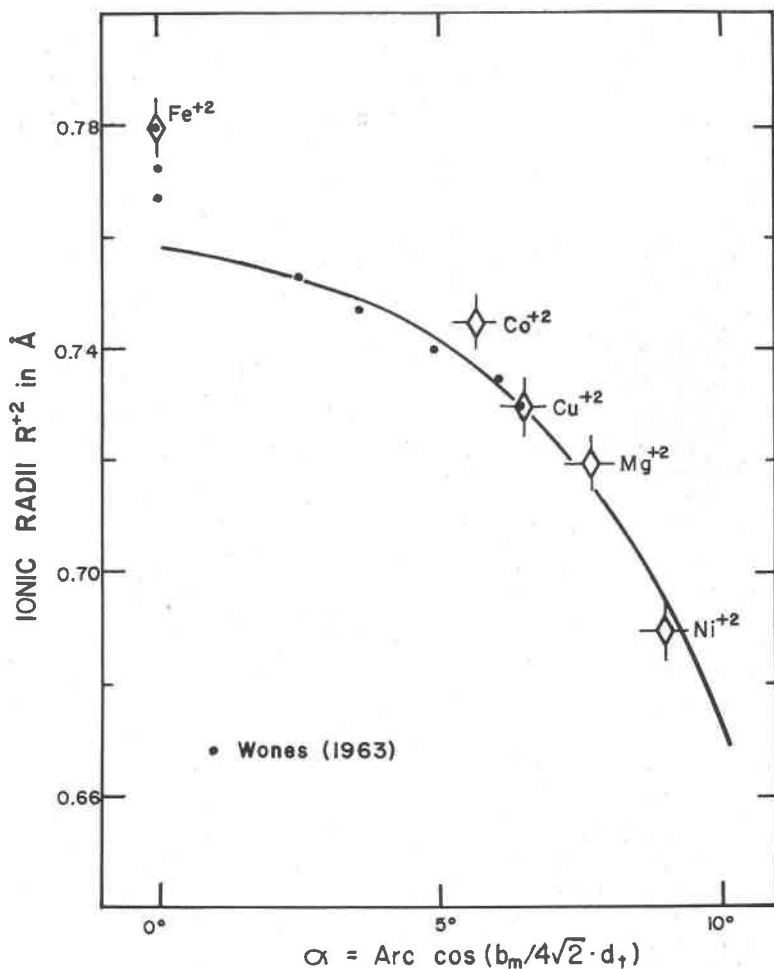


FIG. 9. Tetrahedral layer rotation angle α vs. ionic radius of the octahedral R^{2+} cation for micas of the form $KR_3^{2+}AlSi_3O_{10}(OH)_2$. Black dots represent biotites on the join phlogopite-annite synthesized by Wones (1963b).

known values of b_m , a plot of R^{2+} ionic radius vs. α has been constructed for micas of the form $KR_3^{2+}AlSi_3O_{10}(OH)_2$ (see Fig. 9). As the octahedral cation radius increases to 0.76 Å, α approaches the critical value of 0° . For octahedral cations of ionic radius greater than ≈ 0.76 Å, the tetrahedral layer cannot expand further by rotation. It might therefore be expected that hydrous trioctahedral micas with an $AlSi_3$ tetrahedral layer would not be stable for an octahedral layer cation of radius greater than about 0.76 Å.

OCTAHEDRAL CATION DISTRIBUTION IN NATURAL MICAS

Foster (1960) has plotted the octahedral cation content for over 200 natural phlogopites, biotites, and siderophyllites (Fig. 10). As the Fe^{2+} content of these micas increases, so does the octahedral aluminum content. Trivalent aluminum in R^{2+} sites requires a corresponding substitution of aluminum for silicon in the tetrahedral layer. Thus, aluminum has the dual effect of increasing the size of the tetrahedral layer, while decreasing the effective octahedral cation radius. The maximum observed effective octahedral ionic radius, for the most iron-rich, aluminum-poor specimens, is 0.74 Å. Similarly, mangano-phyllites are known with almost 20 percent MnO substituting for MgO (Jakob, 1925), resulting in an effective octahedral ionic radius of 0.74 Å. Thus, while octahedral cations in natural micas of the form $\text{KR}^{2+}\text{AlSi}_3\text{O}_{10}(\text{OH})_2$ approach the critical ionic radius of 0.76 Å, they are not observed to exceed this value.

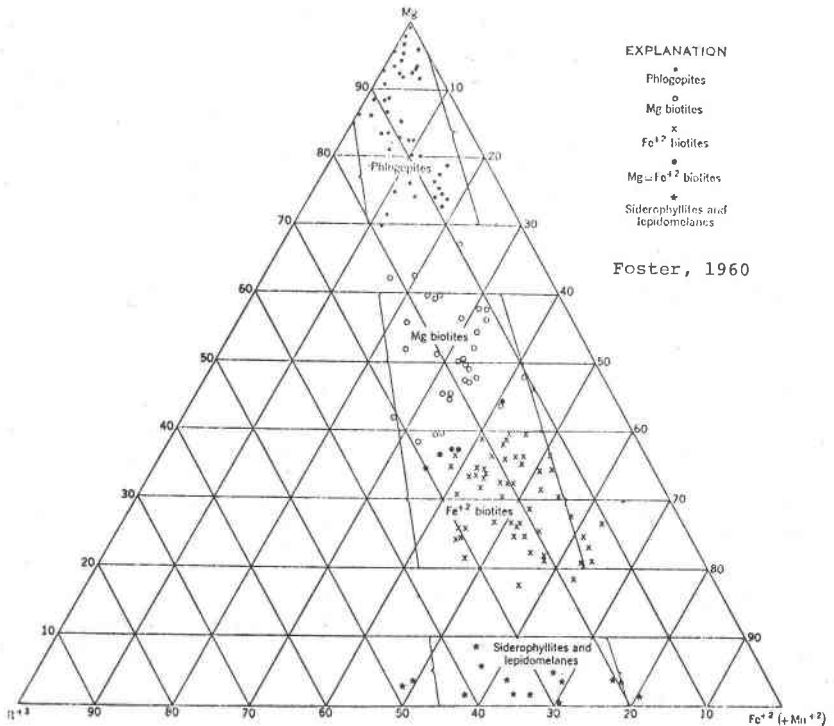


FIG. 10. The composition of the octahedral layer of more than 200 natural phlogopites, biotites, siderophyllites, and lepidomelanes from Foster (1960).

THE COMPOSITION OF ANNITE

Synthetic annite was noted to be the only hydrous trioctahedral mica of the form $KR_3^{2+}AlSi_3O_{10}(OH)_2$ which appears to have an average octahedral ionic radius greater than the critical value of 0.76 Å. Eugster and Wones (1962) have demonstrated that trivalent iron (octahedral ionic radius = 0.63 Å) may substitute for octahedral divalent iron (0.78 Å) in annite as expressed by the oxyannite reaction:



An annite with ≈ 12 mole percent octahedral Fe^{3+} (*i.e.*, ≈ 18 mole percent oxyannite) has an average octahedral cation radius of 0.76 Å, and it was thus predicted that even the most reduced synthetic annites may have appreciable oxyannite content. Subsequent study by Wones, Burns, and Carroll (1971) employing Mössbauer and analytical chemistry techniques have confirmed that at least 10 mole percent of octahedral iron in all synthetic annites is in the trivalent state. It therefore appears that octahedral cation size restrictions, resulting from the misfit between octahedral and tetrahedral mica layers, may have a profound effect on the valency of iron in annite.

From Figure 9 it can be seen that for synthetic biotites of high iron content, tetrahedral rotation (*i.e.*, α) is zero. Therefore, from Donnay, Donnay, and Takeda (1963):

$$\cos \alpha = 1 = b_m/4 \cdot (2)^{1/2} d_t$$

for these micas. However, Wones (1963b) has shown that values for b_m increase with increasing Fe content, in these high-iron biotites. It must therefore be assumed that d_t is also increasing in order to maintain the relation $b_m/d_t = 4(2)^{1/2}$ for these micas. One possible way to increase the mean tetrahedral bond length d_t is by substitution of Fe^{3+} for Al^{3+} in the tetrahedral layer. Since b_m for annite = 9.348 Å, then $d_t = 9.348/4(2)^{1/2} = 1.652$ Å. Donnay, Donnay, and Takeda (1964) have suggested a value of 1.68 Å for d_t of the $FeSi_3$ tetrahedral layer, as opposed to the smaller 1.643 Å mean tetrahedral bond length for an $AlSi_3$ sheet. Therefore, $d_t = 1.652$ implies a composition of $(Fe_{0.2}^{3+}, Al_{0.8}^{3+})Si_3$ (*i.e.*, ≈ 7 percent total iron is trivalent and in tetrahedral sites) for annites' tetrahedral layer. Indeed, Mössbauer studies by Burns (see Wones, Burns, and Carroll, 1971) confirm that 6.5 percent total Fe is tetrahedral Fe^{3+} !

PREDICTION OF TRIOCTAHEDRAL MICA STABILITY

It has been shown that b_m is proportional to the octahedral cation radius (Fig. 1). But we know that $\cos \alpha$ is proportional to b_m/d_t .

Therefore, $\cos \alpha$ is proportional to octahedral ionic radius/ d_t . This linear relation is demonstrated in Figure 11, a plot of $\cos \alpha$ vs. R^{2+} ionic radii for varying mean tetrahedral bond length d_t . The line for an AlSi_3 tetrahedral layer ($d_t = 1.643$) has been developed previously (Fig. 9). Donnay, Donnay, and Takeda (1964) suggest a value of $d_t = 1.68 \text{ \AA}$ for the FeSi_3 tetrahedral layer, and this value has been used to obtain a second line on Figure 11 defined by Ni^{2+} , Mg^{2+} , Co^{2+} , and Fe^{2+} ferri-phlogopites. By noting that these two lines are parallel, and by calculating additional mean tetrahedral bond lengths from data of

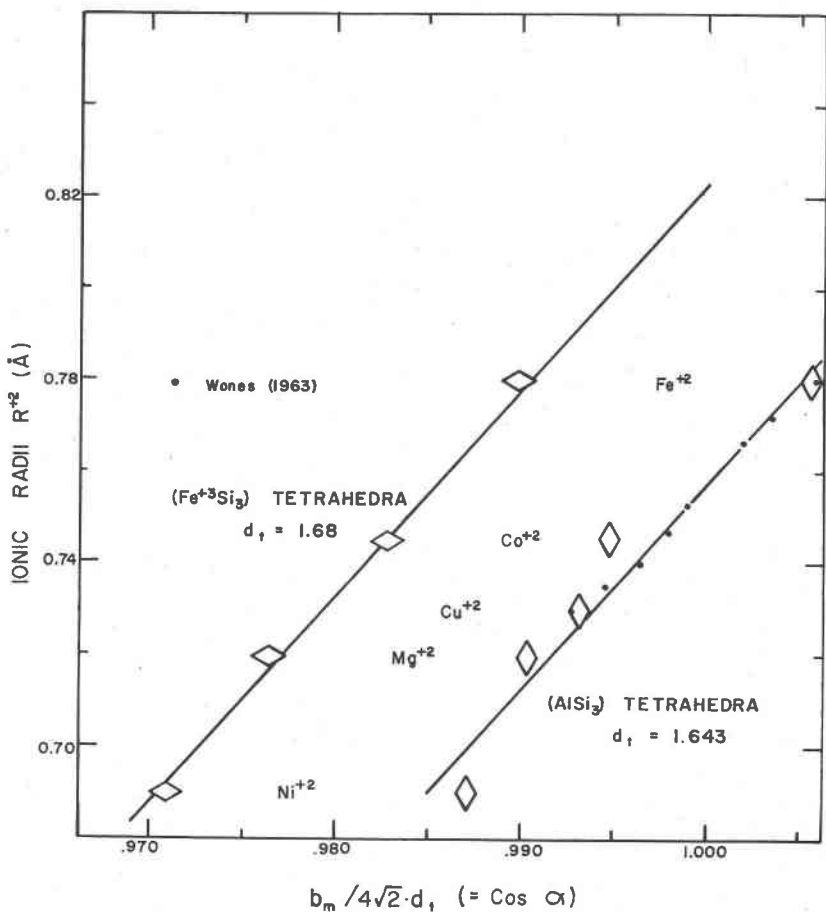


FIG. 11. Cosine of the tetrahedral layer rotation angle α vs. octahedral R^{2+} cation radius for micas of the form $\text{KR}_3^{2+}(\text{AlSi}_3)\text{O}_{10}(\text{OH})_2$ [$d_t = 1.643$] and $\text{KR}_3^{2+}(\text{FeSi}_3)\text{O}_{10}(\text{OH})_2$ [$d_t = 1.68$].

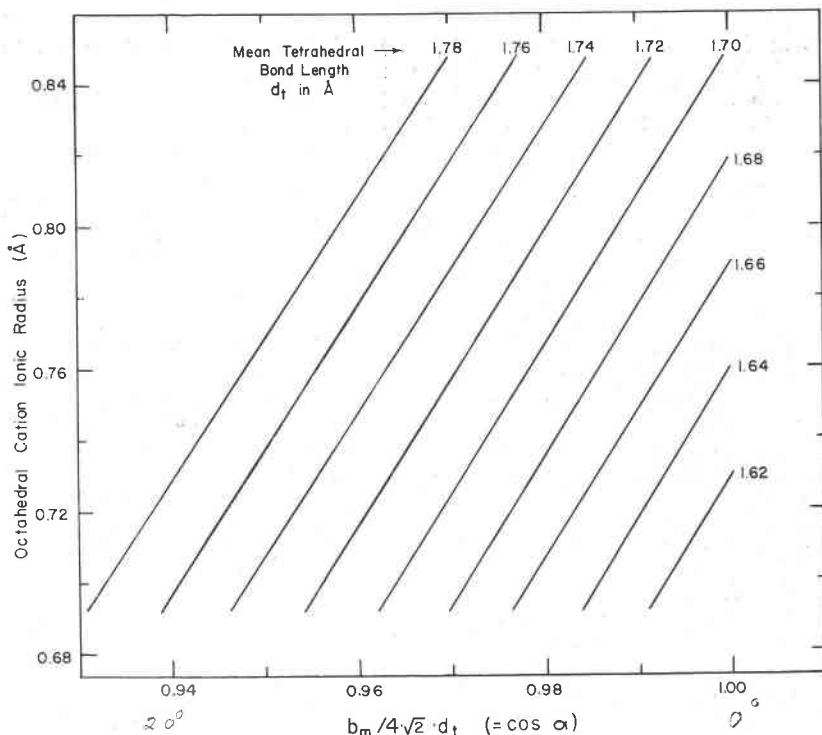


FIG. 12. A nomogram for $\cos \alpha$ vs. octahedral R^{2+} cation radius vs. mean tetrahedral bond length for all hydrous, potassic, trioctahedral micas.

Shannon and Prewitt (rev. 1970), additional lines can be drawn for the BSi_3 , GaSi_3 , and AlGe_3 tetrahedral layers. The resulting nomogram is found in Figure 12. The intersection of any line with $\cos \alpha = 1.00$ defines the critical octahedral cation radius for a hydrous trioctahedral mica with a mean tetrahedral bond length corresponding to that line. Thus, if the composition of a hydrous trioctahedral mica is known, systematic relations between composition and ionic radii enable us to predict unit cell dimensions, structural parameters, and even the stability of the mica.

ACKNOWLEDGMENTS

The authors wish to express their deep appreciation to Dr. Charles W. Burnham and Dr. Hiroshi Takeda for their careful reviews of this study. Their many comments and suggestions have greatly improved the quality of this work. Many thanks are also due to Dr. James Munoz and Dr. Charles T. Prewitt for their stimulating discussions and helpful advice.

Messrs. Robert Charles, Joseph Chernovsky, Yves Pelletier, and Dr. David

Hewitt aided in many aspects of laboratory techniques and maintenance. Many hours of labor were saved through their suggestions and aid. Finally, we wish to thank Mrs. Betsy McCrory for her careful help in preparation of the manuscript.

This investigation was supported by National Science Foundation grants GA1109 and GA13092 to Dr. David R. Wones.

REFERENCES

- BURNHAM, C. W., AND E. W. RADOSLOVICH (1964) Crystal structures of coexisting muscovite and paragonite. *Carnegie Inst. Wash. Yearbook* 63, 232-236.
- BURNS, R. G. (1970) *Mineralogical Applications of Crystal Field Theory*. Cambridge University Press, Cambridge, England, 224 p.
- CARMAN, J. H. (1969) *The Study of the System NaAlSiO₄-Mg₂SiO₄-SiO₂-H₂O from 200 to 5000 bars and 800°C to 1100°C and Its Petrologic Applications*. Ph.D. Thesis, Penn. State Univ. 290 p.
- CROWLEY, M. S., AND R. ROY (1960) The effect of formation pressure on sheet structures—a possible case of Al-Si ordering. *Geochim. Cosmochim. Acta* 18, 94-100.
- DEVRIES R. C., AND R. ROY (1958) The influence of ionic substitution on the stability of micas and chlorites. *Econ. Geol.* 53, 958-965.
- DONNAY, G., J. D. H. DONNAY, AND H. TAKEDA (1964) Trioctahedral one-layer micas. II. Prediction of the structure from composition and cell dimensions. *Acta Crystallogr.* 17, 1371-1381.
- EDISON, T. A. (1916) Precipitation of nickel and cobalt hydroxide. *U.S. Pat. #1,167,484*. [*Chem. Abstr.* 10, 725 (1916)].
- EUGSTER, H. P. (1957) Heterogeneous reactions involving oxidation and reduction at high pressures and temperatures. *J. Chem. Phys.* 26, 1160.
- , AND J. MUNOZ (1966) Ammonium micas: Possible sources of atmospheric ammonia and nitrogen. *Science* 151, 683-686.
- , AND D. R. WONES (1962) Stability relations of the ferruginous biotite, annite. *J. Petrology* 3, 82-125.
- , AND T. L. WRIGHT (1960) Synthetic hydrous boron micas. *U.S. Geol. Surv. Prof. Pap.* 400, B441-B442.
- EVANS, H. T., JR., D. E. APPLEMAN, AND D. S. HANDWERKER (1963) The last squares refinement of crystal unit cells with powder diffraction data by an automatic computer indexing method (abstr) *Amer. Crystallogr. Assoc., Cambridge, Mass., Ann. Meet., Program.* p. 42-43.
- FOSTER, M. D. (1960) Interpretation of the composition of Trioctahedral micas. *U.S. Geol. Surv. Prof. Pap.* 354-B, 11-46.
- FRANZINI, M. (1963) On the crystal structure of biotite. *Z. Kristallogr.* 119, 297-309.
- FRONDEL, C., AND J. ITO (1966) Hendricksite, a new species of mica. *Amer. Mineral.* 51, 1107-1123.
- GLADSTONE, J. H., AND T. P. DALE (1864) Researches on the refraction, dispersion, and sensitiveness of liquids. *Phil. Trans. Roy. Soc. London* 153, 337-348.
- GÜVEN, N. (1967) The crystal structure of 2M₁ phengite and 2M₁ muscovite. *Carnegie Inst. Wash. Yearbook* 66, 487-492.
- HATCH, R. A., R. A. HUMPHREY, W. EITEL, AND J. E. COMEFORO (1957) Synthetic mica investigations. IX. Review of progress from 1947-1955. *U. S. Bur. Mines, Rep. Inv.* 5337.
- JAFFE, H. W. (1956) Application of the rule of Gladstone and Dale to minerals. *Amer. Mineral.* 41, 757-777.

- JAKOB, J. (1925) Beiträge zur chemischen konstitution der glimmer. I. Mitteilung: die schwedischen manganophylle. *Z. Kristallogr.* 61, 155.
- KLINGSBERG, C., AND R. ROY (1957) Synthesis, stability and polytypism of nickel and gallium phlogopite. *Amer. Mineral.* 42, 629-634.
- LARSEN, E. S., AND H. BERMAN (1934) The microscopic determination of the nonopaque minerals. *U.S. Geol. Surv. Bull.* 848, 266 p.
- MCCAULEY, J. W. (1968) *Crystal Structures of the Micas $KMg_2AlSi_6O_{10}F_2$ and $BaLiMg_2AlSi_6O_{10}F_2$* . Ph.D. Thesis, Penn. State Univ., 180 p.
- NEUMANN, H. (1949) Notes on the mineralogy and geochemistry of zinc. *Mineral. Mag.* 28, 575-581.
- RADOSLOVICH, E. W., AND K. NORRISH (1962) The cell dimensions and symmetry of layer lattice silicates. I. Some structural considerations. *Amer. Mineral.* 47, 599-616.
- SCHAIRER, J. F., AND N. L. BOWEN (1955) The system $K_2O-Al_2O_3-SiO_2$. *Amer. J. Sci.* 253, 681-746.
- SEIFERT, F., AND W. SCHREYER (1971) Synthesis and stability of micas in the system $K_2O-MgO-SiO_2-H_2O$ and their relation to phlogopite. *Contrib. Mineral. Petrology* 30, 196-215.
- SHANNON, R. D., AND C. T. PREWITT (1970) Revised values of effective ionic radii. *Acta Crystallogr.* 26, 1046-1048.
- SHAW, H. (1963) The four-phase curve sanidine-quartz-liquid-gas between 500 and 4000 bars. *Amer. Mineral.* 48, 883-896.
- SMITH, J. V., AND H. S. YODER (1965) Experimental and theoretical studies of the mica polymorphs. *Mineral. Mag.* 31, 209-235.
- STEINFINK, H. (1962) Crystal structure of a trioctahedral mica: phlogopite. *Amer. Mineral.* 47, 886-896.
- STUBICON, V., AND R. ROY (1962) Boron substitution in synthetic micas and clays. *Amer. Mineral.* 47, 1166-1173.
- TAKEDA, H., AND C. W. BURNHAM (1969) Fluor-polyolithionite: A lithium mica with nearly hexagonal $(Si_2O_6)^2$ ring. *Mineral. J.* 6, 102-109.
- , AND N. MORIMOTO (1970) Crystal chemistry of rock-forming silicates. II. Structural changes in solid solutions. *J. Crystallogr. Soc. Jap.* 12, 231-248, [in Japanese].
- TUTTLE, O. F. (1949) Two pressure vessels for silicate-water studies. *Geol. Soc. Amer. Bull.* 60, 1727-1729.
- WISE, W. S., AND H. P. EUGSTER (1964) Celadonite: Synthesis, thermal stability and occurrence. *Amer. Mineral.* 49, 1031-1083.
- WONES, D. R. (1963a) Phase equilibria of "ferriannite," $KFe^{+2}Fe^{+3}Si_3O_{10}(OH)_2$. *Amer. J. Sci.* 261, 581-596.
- (1963b) Physical properties of synthetic biotites on the join phlogopite-annite. *Amer. Mineral.* 48, 1300-1321.
- (1967) A low pressure investigation of the stability of phlogopite. *Geochim. Cosmochim. Acta* 31, 2248-2253.
- , R. BURNS, AND B. CARROLL (1971) Stability and properties of annite. (abs.) *Trans. Amer. Geophys. Union* 52, 369-370.
- , AND H. P. EUGSTER (1965) Stability of biotite: Experiment, theory and application. *Amer. Mineral.* 50, 1228-1272.
- YODER, H. S., AND H. P. EUGSTER (1954) Phlogopite synthesis and stability range. *Geochim. Cosmochim. Acta* 6, 157-185.